Catalytic mechanism of fatty acid photodecarboxylase: on the detection and stability of the initial carbonyloxy radical intermediate

Alexey Aleksandrov, Adeline Bonvalet, Pavel Müller, Damien Sorigué, Fred Beisson, Laura Antonucci, Xavier Solinas, Manuel Joffre, Marten Vos

▶ **To cite this version:**

Alexey Aleksandrov, Adeline Bonvalet, Pavel Müller, Damien Sorigué, Fred Beisson, et al.. Catalytic mechanism of fatty acid photodecarboxylase: on the detection and stability of the initial carbonyloxy radical intermediate. Angewandte Chemie International Edition, 2024, 63 (19), pp.e202401376. 10.1002/anie.202401376 . hal-04500852

HAL Id: hal-04500852
https://hal.science/hal-04500852

Submitted on 12 Mar 2024

HAL is a multi-disciplinary open access archive for the deposit and dissemination of scientific research documents, whether they are published or not. The documents may come from teaching and research institutions in France or abroad, or from public or private research centers.

L'archive ouverte pluridisciplinaire **HAL**, est destinée au dépôt et à la diffusion de documents scientifiques de niveau recherche, publiés ou non, émanant des établissements d'enseignement et de recherche français ou étrangers, des laboratoires publics ou privés.

COMMUNICATION

Catalytic Mechanism of Fatty Acid Photodecarboxylase: on the Detection and Stability of the Initial Carbonyloxy Radical Intermediate

Alexey Aleksandrov* [a], Adeline Bonvalet[a], Pavel Müller[b], Damien Sorigué[c], [d], Fred Beisson[c], Laura Antonucci[a], Xavier Solinas[a], Manuel Joffre[a] and Marten H. Vos* [a]

[a] LOB, CNRS, INSERM, École Polytechnique, Institut Polytechnique de Paris, 91120 Palaiseau, France. E-mail: alexey.aleksandrov@polytechnique.edu, marten.vos@polytechnique.edu
[b] Université Paris-Saclay, CEA, CNRS, Institute for Integrative Biology of the Cell (I2BC), 91198 Gif-sur-Yvette, France
[c] Aix-Marseille University, CEA, CNRS, Institute of Biosciences and Biotechnologies, BIAM Cadarache, 13108 Saint-Paul-lez-Durance, France
[d] Department of Chemistry, Princeton University, Princeton, NJ, 08544 USA

Supporting information for this article is given via a link at the end of the document

Abstract: In fatty acid photodecarboxylase (FAP), light-induced formation of the primary radical product RCOO• from fatty acid $RCOO^-$ occurs in 300 ps, upon which CO_2 is released quasi-immediately. Based on the hypothesis that aliphatic RCOO• (spectroscopically uncharacterized because unstable) absorbs in the red similarly to aromatic carbonyloxy radicals such as 2,6-dichlorobenzoyloxy radical (DCB•), much longer-lived linear RCOO• has been suggested recently. We performed quantum chemical reaction pathway and spectral calculations. These calculations are in line with the experimental DCB• decarboxylation dynamics and spectral properties and show that in contrast to DCB•, aliphatic RCOO• radicals a) decarboxylate with a very low energetic barrier and on the timescale of a few ps and b) exhibit little red absorption. A time-resolved infrared spectroscopy experiment confirms very rapid, <<300 ps RCOO• decarboxylation in FAP. We argue that this property is required for the observed high quantum yield of hydrocarbons formation by FAP.

In photoenzymes, bound substrates are transformed to products in reaction sequences initiated by the absorption of a photon by the enzyme. Photoenzymes are of high fundamental interest because they allow identification of short-lived intermediates in real time using short light pulses, on time scales that are not accessible in diffusion-limited catalytic reactions[1]. Furthermore, photoenzymes are increasingly recognized as promising catalysts in green chemistry applications[1-5]. Presently, there are only three known distinct types of natural photoenzymes. Of these, fatty acid photodecarboxylase (FAP) is a flavoenzyme that transforms fatty acids into hydrocarbons and CO_2 with high (70 – 80%) photochemical quantum yield (QY)[6-7]. Since its discovery in 2017[6], FAP has become the subject of intense research, aiming to both unravel its fundamental mechanism[6, 8-10] and explore its potential as a template for novel green chemistry photocatalytic reactions[11]. These research lines are intertwined, as understanding the mechanism is essential for the design of derived photocatalysts.

Structural characterization of the enzyme-substrate complex[6] from *Chlorella variabilis* FAP (*Cv*FAP) has revealed the proximity of the fatty acid COO^- group to the isoalloxazine chromophore of the flavin adenine dinucleotide (FAD) cofactor, with a ring-to-oxygen distance of ~3.2 Å. The electronic excited state ^{1}FAD*, which is populated following photon absorption, decays in ~300 ps (τ_1 in Scheme 1), leading to the formation of the flavosemiquinone radical $FAD^{\bullet-}$, as inferred from transient fluorescence and absorption spectroscopy. The required electron is donated by the fatty acid substrate; in its absence, ^{1}FAD* decays by its intrinsic decay in ~5 ns, with a high yield of the triplet state ^{3}FAD*[6]. Unsurprisingly, *Cv*FAP's structure does not display aromatic residues near the FAD cofactor that typically serve as intrinsic photoprotective electron donors in non-photoactive flavoproteins[12]. Such residues could lead to QY-reducing reactions competing with catalysis in FAP. The oxidized substrate radical resulting from the 300-ps electron transfer (ET) reaction is of the form RCOO• (where R stands for the linear/aliphatic hydrocarbon chain), presumably the direct precursor to CO_2 release.

$$^1FAD^* \quad RCOO^- \xrightarrow{\tau_1} FAD^{\bullet-} \quad RCOO^{\bullet} \xrightarrow{\tau_2} FAD^{\bullet-} \quad R^{\bullet} + CO_2$$

Scheme 1. First two steps of the FAP reaction cycle after population of the flavin excited state ^{1}FAD*.

The ensuing reaction mechanism has been investigated in detail by a consortium employing an array of experimental and computational techniques[9]. One major conclusion drawn from this work was that CO_2 release from the primary product, RCOO•, occurs with the same 300-ps time constant as ET, implying that this release intrinsically occurs quasi-instantaneously upon ET (τ_2 << 300 ps in Scheme 1). This conclusion was supported by various approaches: a) time-resolved infrared (TR-IR) experiments that kinetically resolved the formation of CO_2, in a background-free spectral range, with a time constant of ~300 ps, b) time-resolved serial femtosecond crystallography (TR-SFX) that demonstrated major loss of electronic density around the carboxyl group of the substrate at 900 ps, consistently indicating that CO_2 formation occurs in less than 1 ns, and c) quantum chemical calculations supporting a barrierless CO_2 dissociation pathway from RCOO• [9]. This assessment is also in general agreement with the high-rate (~10^{12} s^{-1}) and barrierless decarboxylation of long-chain acyloxy radicals, as suggested by the determination of product yields upon thermolysis of precursors using chemically induced dynamic nuclear polarization spectroscopy[13].

The above assessment that the decarboxylated R• reaction intermediate in FAP is formed immediately upon ET in ~300 ps was recently challenged by Zhong and coworkers.[10]. Analyzing single wavelength transient absorption spectroscopic data in *Cv*FAP bound to a palmitic acid substrate in the near infrared to ultraviolet (UV) spectral region, they extracted a small feature that rises in 300 ps and decays in ~5 ns (incidentally also the time constant of ^{1}FAD* decay in substrate-devoid FAP) and that would absorb only in the 700-900 nm range and in the UV. This feature was assigned to RCOO• and correspondingly, τ_2 in Scheme 1 was proposed to be 5 ns. Spectra of RCOO• for linear hydrocarbon chains are not available; therefore this assignment was based on a presumed resemblance to a spectrum of a carbonyloxy radical of an aromatic ring system from the literature, specifically the 2,6-dichlorobenzoyloxy radical (DCB•), obtained by photodissociation of bis-DCB peroxide[14]. Due to their π→π* transitions, derivatives of aromatic compounds are generally more prone to absorb in the Vis/NIR region than those of linear hydrocarbon chains. Therefore, validation of the assumption that the spectral properties are determined basically by the carbonyloxy radical group, which critically underlies the proposed paradigm change, would be warranted. To this end, we performed quantum chemical calculations to assess the stability and spectrum of linear chain RCOO• radicals, specifically hexadecanoyloxy (HDX•) and decanoyloxy (DX•), as well as of the DCB• aromatic model radical (Scheme 2).

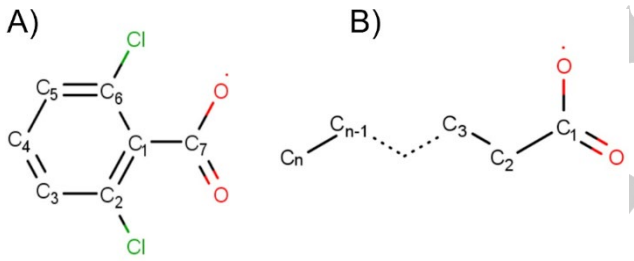

Scheme 2. Radicals studied in this work. A) DCB• and B) HDX• (n=16) and DX• (n=10).

Figure 1 presents reaction profiles in vacuum computed using the HEBS method for HDX• and DX•, as well as DCB• for comparison. With respect to our previous work on HDX•[9], for the linear chain radicals we extended the reaction profile to shorter C1-C2 distances and narrow O1-C1-O2 angles, resulting in a conformation that remains stable during minimization (see SI). To achieve this, starting from the structures of the RCOO$^-$ ground state, minimization of RCOO• was initiated with a constraint on the C1-C2 distance, ensuring it remained below 1.47 Å. Subsequently, minimization proceeded without any further constraints. The resulting optimized geometry for the RCOO• radical exhibited a C1-C2 distance of 1.50 Å, which is shorter than the RCOO$^-$ ground state value of 1.57 Å in vacuum. Consequently, in [9], where RCOO• minimization started using the RCOO$^-$ ground state structure with the C1-C2 distance of 1.57 Å, it led directly to the formation of CO_2 and alkyl radicals due to the longer C1-C2 distance in RCOO$^-$ in vacuum.

For all three systems, a sizeable barrier for CO_2 formation was found (Fig. 1). The energies of reactant, product and transition state structures are given in Table 1. Energies along the reaction profile for the two fatty acid radicals are very similar demonstrating that the alkane chain length does not affect the decarboxylation reaction. In the absence of solvent, the free energy barrier for the decarboxylation reaction is 4.4 kcal·mol^{-1}. When modeled in an aqueous environment using the SMD solvation model, this barrier is reduced to 2.6 kcal·mol^{-1}, as estimated through the implementation of the SMD model. This free energy barrier corresponds to a reaction rate of $8 \cdot 10^{10}$ s^{-1} (τ_2 = 12 ps) at room temperature as estimated using the Eyring equation. For DCB•, much higher barriers are computed (7.1, 12.0, and 10.2 kcal·mol^{-1} in vacuum, water and acetonitrile respectively), and correspondingly experimentally observed for the activation barrier (7.9 kcal·mol^{-1}) and time constant (100 ns) in acetonitrile[15].

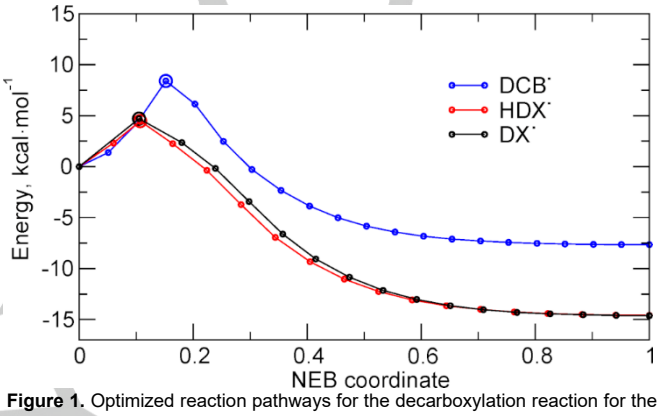

Figure 1. Optimized reaction pathways for the decarboxylation reaction for the DCB•, DX•, and HDX• radicals in vacuum. The structures representing the reaction pathways are shown by dots. The potential energy is given relative to the reactant states. The refined structures for the transition states are encircled.

Table 1. Relative energies (in kcal.mol^{-1}) of product and transition state (TS) structures for decarboxylation of DCB•, HDX• and DX•. Energies are given relative to the reactant state. E_{el} and G are the electronic structure energy and the Gibbs free energy, respectively. G_{water} includes solvation effects computed with the SMD model for water; G_{exp} from reference [14] was measured in acetonitrile

Molecule	State	E_{el}	G	G_{water}	G_{exp}
DCB•	TS	8.4	7.1	12.0	7.9
	product	-7.7	-10.6	-1.4	
HDX•	TS	4.4	4.4	2.6	
	product	-14.6	-20.3	-12.5	
DX•	TS	4.4	4.4	2.7	
	product	-14.6	-18.9	-11.0	

In *Cv*FAP, the computed energy barrier for HDX• decarboxylation is reduced to 2.3 (±0.1) kcal·mol^{-1}, while the resulting product state is 8.0 (±0.4) kcal·mol^{-1} lower in energy than the initial reactant state (Figure 2). To assess the impact of the initial geometry on energies, we performed two independent reaction path calculations, each initiated from distinct sets of coordinates extracted from MD simulations. Remarkably, these calculations yielded close energy profiles, with energy barriers of 2.2 and 2.4 kcal·mol^{-1}, respectively. We further employed a rigid rotor-harmonic oscillator approximation to estimate the entropy contribution. However, these entropy contributions were negligible as they had a minimal impact on energy values, causing

changes of less than 0.1 kcal·mol^{-1}. Overall, the decarboxylation reaction barrier after ET in FAP closely matches the 2.6 kcal·mol^{1} barrier computed in solvent. Therefore, the protein environment does not significantly change the activation energy relative to the solvent. The free energy of 2.3 kcal·mol^{-1} corresponds to a reaction rate of $1.3 \cdot 10^{11}$ s^{-1} (τ_2 = 8 ps) estimated using the Eyring equation. This finding strongly suggests that the decarboxylation reaction in FAP occurs on a much shorter timescale than the preceding (τ = 300 ps) electron transfer reaction, thus precluding the significant accumulation of the RCOO• radical state.

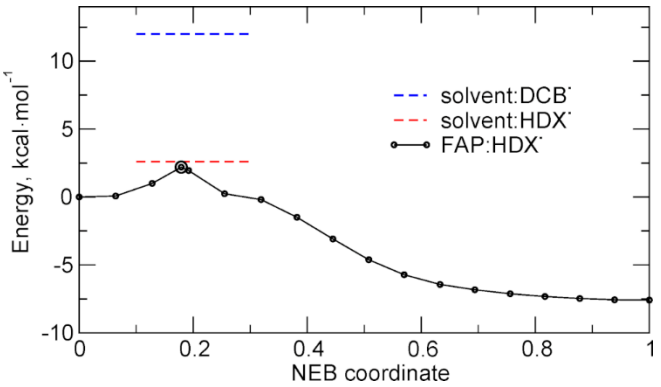

Figure 2. Optimized reaction pathways for the decarboxylation reaction of the HDX• radical in FAP. The dashed lines show the computed barriers for the HDX• and DCB• radicals within the solvent. The structures representing the reaction pathways are indicated by dots, and the potential energy is given relative to the reactant states. The refined structure for the transition states is encircled.

The relatively low activation energy for the decarboxylation reaction in FAP and solvent can be attributed to the fact that the reactant state is structurally very close to the transition state. In particular, the crucial bond distance between C1 and C2 in the PCX• radical within FAP is 1.48 Å in the reactant state and 1.52 Å in the transition state.

Together, these reaction pathway calculations demonstrate that decarboxylation of carbonyloxy radical compounds occurs with much lower barriers for linear-chain than for aromatic compounds. In particular, they predict decarboxylation on the nanosecond timescale for DCB• in solution, as experimentally observed, and in a few picoseconds for linear-chain HDX• in FAP. The latter finding is incompatible with the suggestion of nanosecond-lived HDX• in FAP in Ref. [10]. Our results are in general agreement with previous theoretical work showing that insertion of a CH_2 group between the benzene and the carboxyl group of the benzoyloxy radical (thus 'linearizing' its direct environment) results in a significant reduction in the stability[16-17]. Benzoyloxy radicals like DCB• can be stabilized by delocalization ('resonance') of the unpaired electron over multiple carbon atoms forming the π-system and are hence quite stable towards decarboxylation in their ground-state, quantitatively explaining lifetimes in the ns-to-ms range at ambient temperatures[16].

We now turn to the spectral properties of the carbonyloxy radical compounds. Figure 3 shows the vacuum absorption spectra for DX•, HDX•, and DCB•. The DCB• spectrum is dominated by a band at ~620 nm and includes one further band in the near IR characterized by lower intensity. This finding is in good agreement with the broad experimental absorption spectra displaying maxima at ~700 nm in acetonitrile and ~650 nm in tetrachloromethane[14]. In the red/near-IR region DX• and HDX• exhibit an identical absorption, centered at 670 nm, that is more than 3-fold weaker than that of the aromatic compound DCB•. In addition, all three radicals also absorb in the 300-450 nm wavelength range.

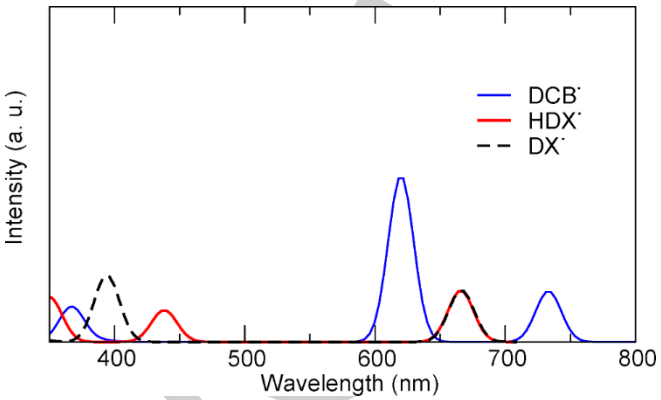

Figure 3. Calculated absorption spectra for the DCB•, DX• and HDX•, radicals in vacuum.

Spectra of the hypothetical RCOO• radical within the *Cv*FAP protein were generated based on the analysis of structures extracted from 100-ns MD simulations of the *Cv*FAP ground state. Among the initial pool of 100 structures selected for spectral calculations, three structures exhibiting spontaneous decarboxylation, marked by the presence of CO_2 and an alkyl radical, were excluded from further analysis. Consequently, our final spectra for the hypothetical hexadecanoyloxy radical in *Cv*FAP were generated by averaging data derived from 97 distinct geometries. Fig. 4 displays the calculated absorption spectrum for HDX• within the *Cv*FAP protein environment, which shows a modest blue shift of 20 nm with respect to vacuum, resulting in a central wavelength of 645 nm, and band broadening due to the heterogeneous environment. For comparison, Fig. 4 also displays calculations for FAD_{ox} absorption within the *Cv*FAP protein complex using the same 97 structures and Gaussian width parameters. Overall, the absorbance of HDX• in the 600-700 nm region is far weaker than that of FAD_{ox} in the 400-500 nm region (the area under the absorption bands is 22 times larger for FAD_{ox}).

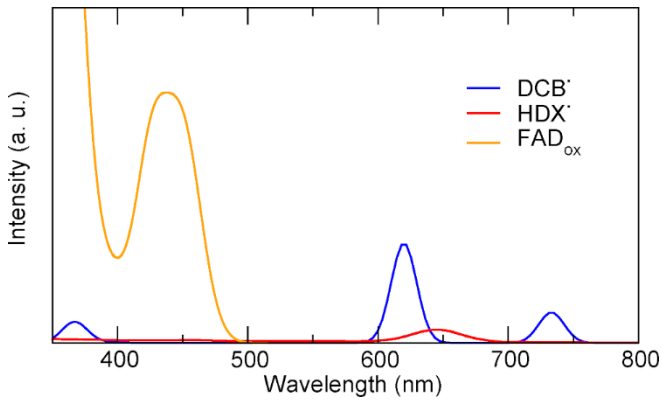

Figure 4. Calculated absorption spectra for the HDX• radical and FAD_{ox} within the *Cv*FAP protein environment and that of with DCB• in a vacuum.

For the DCB• radical, the Natural Transition Orbitals (NTOs)[18] associated with the transition corresponding to the absorption near 620 nm shown in Fig. S1, reveal that the excitation involves mostly π-bonding character in the hole NTO and π-antibonding interactions between the carbon of the

benzene and the carboxyl group in the particle NTO. For the HDX• radical, the peak near 670 nm is remarkably similar across saturated fatty acids of various chain lengths, as detailed in Table S1. This finding can be attributed to the localized nature of the electronic transition as demonstrated in Figure S1. Similar to the transition in the DCB• radical, the transitions in the HDX• radical involve orbitals that have a bonding character between the carbon C2 of the alkyl part and the C1 atom of the carboxyl group in the hole NTO and antibonding character in the excited state.

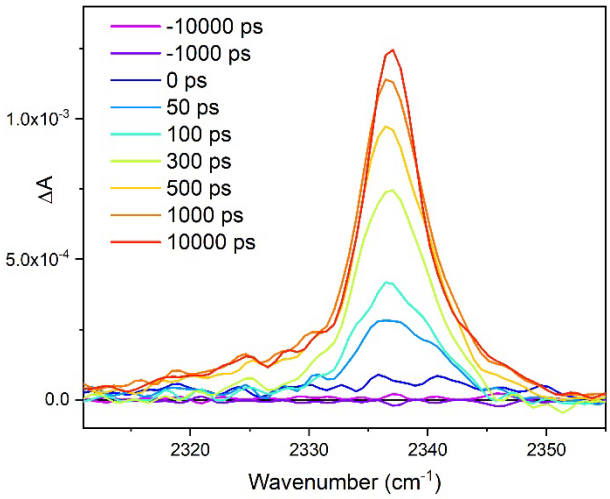

Figure 5. Transient spectra in the CO_2 absorption region at different delay times upon excitation of *Cv*FAP reflecting decarboxylation of the substrate. The spectra peak at 2337.5 cm^{-1}, which is shifted with respect to the value in aqueous solution [19], 2342 cm^{-1} due to the protein environment[9].

The above computational results strongly indicate that the intermediate feature extracted from the data of Ref. [10] cannot be assigned to formation and decay of a linear-chain RCOO• radical. We note that the 5-ns decay time of this feature coincides with that of ^{1}FAD* decay in the fraction (as high as 20% in Ref.[10]) of the sample that does not bind substrate, but that the subtraction procedure to take into account this fraction is not detailed. As outlined above, our previous TRIR experiments, supported by TR-SFX and calculations, have shown that RCOO• decarboxylation occurs in ~300 ps, *i.e.*, quasi concomitant with RCOO• formation[9]. New TRIR experiments with further improved signal-to-noise ratio (Fig. 5) further strengthen this assessment. We also note that the visible transient absorption remaining after the ~300 ps phase in the 600-660 range consists of a broad featureless induced absorption ~40 times lower than that of the bleaching of the FAD_{ox} band and that no induced absorption band around 645 nm with an amplitude exceeding 1% of the FAD_{ox} band bleaching can be discerned (Fig. S8 of Ref. [9]). Together with the above calculation of the HDX• spectrum at ~645 nm in *Cv*FAP being ~22 times lower than the FAD_{ox} absorption, this assessment is fully consistent with the lack of any RCOO• population predicted by the quasi-instantaneous (<<300 ps) CO_2 release upon RCOO• formation. Altogether, our computational and time-resolved spectroscopic results clearly show that decarboxylation occurs predominantly before 1 ns and not between 1 ns and 10 ns as proposed by Zhong and coworkers[10].

Our simulations demonstrate that, in contrast to aromatic benzoyloxy radicals, decarboxylation of aliphatic RCOO• radicals occurs with a low barrier on the timescale of a few picoseconds. This property has important consequences for the functioning of FAP. The [FAD•⁻ RCOO•] initial product state has been calculated to lie only slightly lower than its precursor state [^{1}FAD* RCOO⁻] [9]; i.e. almost iso-energetic. Competing with decarboxylation of RCOO•, wasteful back ET to the resting ground state [FAD RCOO⁻] can occur either directly or via the ^{1}FAD* excited state. The direct [FAD•⁻ RCOO•] → [FAD RCOO⁻] back reaction has a very large driving force (2.65 eV) but assuming a typical reorganization energy of the order of 0.7 to 1 eV[20] could take place in the Marcus inverted region[21] with a large activation barrier and therefore presumably be slow. However, back ET to the ^{1}FAD* excited state [FAD•⁻ RCOO•] → [^{1}FAD* RCOO⁻] is expected to occur much faster, in ~2 ns given the forward ET of ~300 ps and the calculated 1.1 kcal.mol^{-1} energy difference between these states[9]. As the ^{1}FAD* state has an intrinsic lifetime of ~5 ns, decarboxylation on the timescale of a few nanoseconds would be detrimental to quantum yield of the photoreaction. This reasoning is illustrated in the reaction scheme (Fig. 6), summarizing the energetics and kinetics of the initial reaction steps of the FAP photocycle.

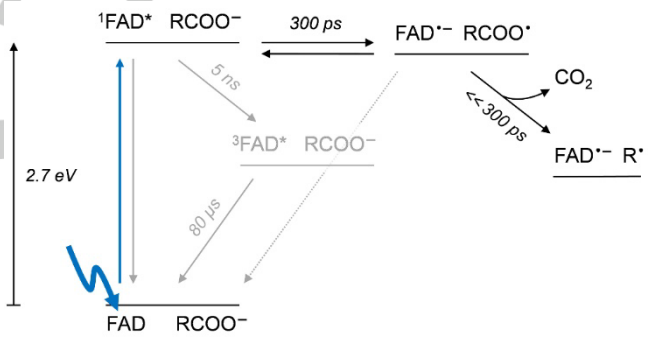

Figure 6. Initial reaction steps and competing futile back reactions in the photocycle of *Cv*FAP.

Acknowledgements

We thank Antonio Monari (Université Paris Cité) for very helpful discussions and we acknowledge the ANR grant 18-CE11-0021. D.S. was supported by a Marie Sklodowska-Curie Actions global fellowship (Project 101063280 - EXPERIMENTAL).

Keywords: photoenzyme ● ultrafast spectroscopy ● quantum simulations ● radical ● reaction pathway

[1] A. Taylor, D. J. Heyes, N. S. Scrutton, *Curr. Opin. Struct. Biol.* **2022**, *77*, 102491.
[2] W. Harrison, X. Huang, H. Zhao, *Acc. Chem. Res.* **2022**, *55*, 1087-1096.
[3] L.-E. Meyer, B. E. Eser, S. Kara, *Curr. Opin. Green Sust. Chem.* **2021**, *31*, 100496.
[4] L. Schmermund, V. Jurkaš, F. F. Özgen, G. D. Barone, H. C. Büchsenschütz, C. K. Winkler, S. Schmidt, R. Kourist, W. Kroutil, *ACS Catal.* **2019**, *9*, 4115-4144.
[5] M. A. Emmanuel, S. G. Bender, C. Bilodeau, J. M. Carceller, J. S. DeHovitz, H. Fu, Y. Liu, B. T. Nicholls, Y.

Ouyang, C. G. Page, T. Qiao, F. C. Raps, D. R. Sorigué, S.-Z. Sun, J. Turek-Herman, Y. Ye, A. Rivas-Souchet, J. Cao, T. K. Hyster, *Chem. Rev.* **2023**, *123*, 5459-5520.

[6] D. Sorigué, B. Légeret, S. Cuiné, S. Blangy, S. Moulin, E. Billon, P. Richaud, S. Brugière, Y. Couté, D. Nurizzo, P. Müller, K. Brettel, D. Pignol, P. Arnoux, Y. Li-Beisson, G. Peltier, F. Beisson, *Science* **2017**, *357*, 903-907.

[7] P. P. Samire, B. Zhuang, B. Légeret, Á. Baca-Porcel, G. Peltier, D. Sorigué, A. Aleksandrov, F. Beisson, P. Müller, *Sci. Adv.* **2023**, *9*, eadg3881.

[8] D. J. Heyes, B. Lakavath, S. J. O. Hardman, M. Sakuma, T. M. Hedison, N. S. Scrutton, *Acs Catal.* **2020**, *10*, 6691-6696.

[9] D. Sorigué, K. Hadjidemetriou, S. Blangy, G. Gotthard, A. Bonvalet, N. Coquelle, P. Samire, A. Aleksandrov, L. Antonucci, A. Benachir, S. Boutet, M. Byrdin, M. Cammarata, S. Carbajo, S. Cuiné, R. B. Doak, L. Foucar, A. Gorel, M. Grünbein, E. Hartmann, R. Hienerwadel, M. Hilpert, M. Kloos, T. J. Lane, B. Légeret, P. Legrand, Y. Li-Beisson, S. Moulin, D. Nurizzo, G. Peltier, G. Schirò, R. L. Shoeman, M. Sliwa, X. Solinas, B. Zhuang, T. R. M. Barends, J.-P. Colletier, M. Joffre, A. Royant, C. Berthomieu, M. Weik, T. Domratcheva, K. Brettel, M. H. Vos, I. Schlichting, P. Arnoux, P. Müller, F. Beisson, *Science* **2021**, *372*, eabd5687.

[10] R. Wu, X. Li, L. Wang, D. Zhong, *Angew. Chem. Int. Ed.* **2022**, *61*, e202209180.

[11] X. Guo, A. Xia, W. Zhang, Y. Huang, X. Zhu, X. Zhu, Q. Liao, *Bioresour. Technol.* **2023**, *367*, 128232.

[12] B. Zhuang, U. Liebl, M. H. Vos, *J. Phys. Chem. B* **2022**, *126*, 3199-3207.

[13] A. Fraind, R. Turncliff, T. Fox, J. Sodano, L. R. Ryzhkov, *J. Phys. Org. Chem.* **2011**, *24*, 809-820.

[14] J. Wang, T. Tateno, H. Sakuragi, K. Tokumaru, *J. Photochem. Photobiol. A* **1995**, *92*, 53-59.

[15] J. Wang, M. Tsuchiya, H. Sakuragi, K. Tokumaru, H. Itoh, *Tetrahedron Lett.* **1994**, *35*, 6321-6324.

[16] M. Kling, S. Schmatz, *Phys. Chem. Chem. Phys.* **2003**, *5*, 3891-3896.

[17] B. Abel, J. Assmann, P. Botschwina, M. Buback, M. Kling, R. Oswald, S. Schmatz, J. Schroeder, T. Witte, *J. Phys. Chem. A* **2003**, *107*, 5157-5167.

[18] R. L. Martin, *J. Chem. Phys.* **2003**, *118*, 4775-4777.

[19] L. H. Jones, E. McLaren, *J. Chem. Phys.* **1958**, *28*, 995-995.

[20] C. C. Page, C. C. Moser, X. Chen, P. L. Dutton, *Nature* **1999**, *402*, 47-52.

[21] R. A. Marcus, N. Sutin, *Biochim. Biophys. Acta* **1985**, *811*, 265-322.

WILEY-VCH

Entry for the Table of Contents

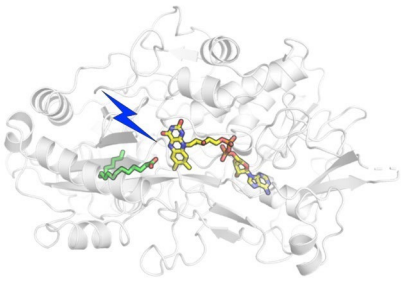

Quantum chemical decarboxylation reaction pathway and spectral calculations of aliphatic and aromatic carbonyloxy radicals demonstrate that they have distinct electronic absorption properties and that the former are much more unstable. These findings pertain to a controversy on the mechanism of the photoenzyme fatty acid photodecarboxylase. They support the here reinforced experimental observation of intrinsic CO_2 dissociation in <<300 ps.

Institute Twitter username: @LabOptBio

WILEY-VCH